DTU Library

High-Spatial-Multiplicity Multicore Fibers for Future Dense Space-Division-Multiplexing Systems

Matsuo, Shoichiro; Takenaga, Katsuhiro; Sasaki, Yusuke; Amma, Yoshimichi; Saito, Shota; Saitoh, Kunimasa; Matsui, Takashi; Nakajima, Kazuhide; Mizuno, Takayuki; Takara, Hidehiko

Total number of authors:
12

High-Spatial-Multiplicity Multicore Fibers for Future Dense Space-Division-Multiplexing Systems

Shoichiro Matsuo, *Member, IEEE, Member, OSA*, Katsuhiro Takenaga, Yusuke Sasaki, Yoshimichi Amma, Shota Saito, Kunimasa Saitoh, *Member, IEEE, Member, OSA*, Takashi Matsui, Kazuhide Nakajima, *Member, IEEE*, Takayuki Mizuno, *Member, IEEE*, Hidehiko Takara, *Member, IEEE*, Yutaka Miyamoto, *Member, IEEE*, and Toshio Morioka, *Member, IEEE, Fellow, OSA*

(Invited Paper)

Abstract—**Multicore fibers and few-mode fibers have potential application in realizing dense-space-division multiplexing systems. However, there are some tradeoff requirements for designing the fibers. In this paper, the tradeoff requirements such as spatial channel count, crosstalk, differential mode delay, and cladding diameter are discussed. Further, the design concept and transmission characteristics of high-core-count single-mode multicore fibers are discussed. A heterogeneous multicore fiber with 30 cores and quasi-single-mode multi-core fibers with 31 cores are developed.**

Index Terms—**Optical fiber, optical fibers communication.**

I. Introduction

SPACE division multiplexing (SDM) over multicore fibers (MCFs) or few-mode fibers (FMFs) has been investigated to overcome the capacity limitation of approximately 100 Tb/s/fiber for the existing optical communication system over a single-mode single-core fiber (SM-SCF). Many SDM transmission experiments over MCFs or FMFs have demonstrated the possibility of SDM technology for future dense SDM systems [1]–[13].

A fiber for SDM is expected to involve as many spatial channels as possible under some restrictions such as cladding diameter, intercore crosstalk (XT), inner-core XT, and differential mode delay (DMD). Many types of single-mode MCFs (SM-MCFs) and FMFs have been proposed to increase core count or mode count. The maximum core count of SM-MCF was beyond 30 [14], [15]. The mode count of FMFs reached 36 (20 LP modes) [16]. Another approach is combining few modes and multiple cores: few-mode multicore fibers (FM-MCFs). Some FM-MCFs exceeded the record spatial channel count (SCC) of SM-MCFs and FMF: 36 with 3 modes × 12 cores [7], [8], 72 with 6 modes × 12 cores [17], 108 with 3 modes × 36 cores [9], 114 with 6 modes × 19 cores [10]. However, FM-MCFs should overcome both issues for SM-MCFs and FMFs simultaneously.

In this paper, we review the features of high-spatial-multiplicity MCFs [18]. At first, the current states of the SDM fiber including FMFs, SM-MCFs, and FM-MCFs are reviewed. The tradeoff relationship between multiplicity and cladding diameter, XT, and DMD is discussed. Then, two studies on SM-MCFs with high spatial multiplicity are presented. The high-spatial-multiplicity fibers are realized using heterogeneous structures or quasi-single-mode (QSM) structures, respectively. The design concept, fabrication results, and transmission performance of the fabricated fibers are presented.

II. Spatial Multiplicity Improvement

In this section, recent approaches regarding SDM fiber for dense SDM are presented. After defining the parameters for comparing multiplicity, the tradeoff parameters for high spatial multiplicity—cladding diameter, core-to-core XT, and DMD—are discussed.

A. SCC and Spatial Efficiency (SE)

In this study, we used the SCC, SE, and relative SE (RSE) as a measure of the spatial multiplicity of MCFs and FMFs.

$$\text{SCC} = \text{CC} \cdot \text{MC}, \tag{1}$$

$$\text{SE} = \frac{\text{SCC}}{(\pi/4) \, D_c^2}, \tag{2}$$

$$\text{RSE} = \frac{\text{SE}_{\text{MCF}}}{\text{SE}_{\text{CSMF}}} = \text{SCC} \cdot \left(\frac{125}{D_c}\right)^2, \tag{3}$$
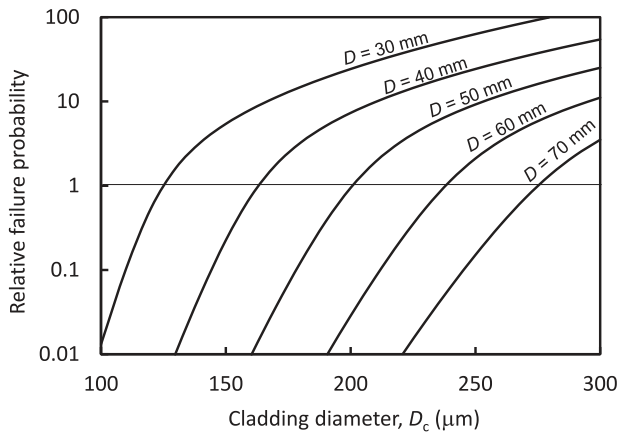
Fig. 1. Relative failure probability as a function of cladding diameter D_c for different bending diameters D. Failure probability was estimated under the condition of 100 turns, 20 years, and 1% proof.

where CC is the core count in a fiber, MC is the mode count in a core, D_c is the cladding diameter of a fiber, $\mathrm{SE_{MCF}}$ is the SE of an MCF, and $\mathrm{SE_{CSMF}}$ is the SE of the conventional single-mode fiber (SMF) with SCC = 1, $A_{\mathrm{eff}} = 80\ \mu\mathrm{m}^2$ at 1550 nm, and $D_c = 125\ \mu\mathrm{m}$.

B. SCC Versus Cladding Diameter

The cladding diameter of most MCFs presented so far is larger than 125 μm, which is the general cladding diameter of SM-SCFs. However, the cladding diameter of MCFs is limited to less than a certain value based on the requirements of the transmission fiber.

The first limiting factor is mechanical reliability. Fig. 1 shows the simulation results of failure probability as a function of the cladding diameter for a different bending diameter D under the condition of 100 turns, 20 years, and 1% proof [19]. Relative failure probability is the failure probability of a fiber with a certain D_c to the failure probability of a fiber with $D_c = 125\ \mu\mathrm{m}$ and $D = 30$ mm. Here, we define the D at which the relative failure probability equals 1 as the allowable bending diameter for a D_c. The allowable bending diameter increases following an increase in the D_c. We should accept an allowable bending diameter larger than 60 mm if the D_c exceeds approximately 250 μm.

The allowable bending diameter can be improved by using a heightened proof level. Fig. 2 shows the relationship between the allowable bending diameter and the proof level for various D_cs. Even for a fiber with $D_c = 300\ \mu\mathrm{m}$, the allowable bending diameter can be reduced to less than 60 mm for a proof level larger than 1.5%. Note that the required stress for a proof test is proportional to $D_c{}^2$ and the proof level. The possibility of high-level proof testing for a large cladding diameter fiber may limit the possible D_c.

Another limiting factor is splice ability. A large cladding diameter implies that the position of the outermost core is far away from the center of the cladding. The splice loss (L_s in [dB]) is given by the following equation [20]:

$$L_s = -10 \log \left(\left(\frac{2w_1 w_2}{w_1^2 + w_2^2} \right)^2 \exp \left(-\frac{2d^2}{w_1^2 + w_2^2} \right) \right), \quad (4)$$
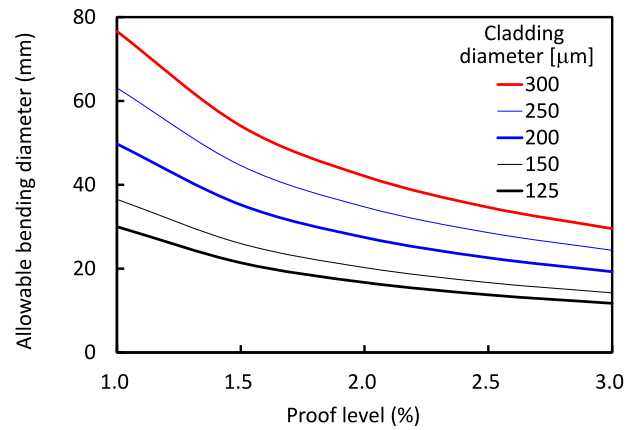
Fig. 2. Allowable bending diameter as a function of proof level for various cladding diameters.
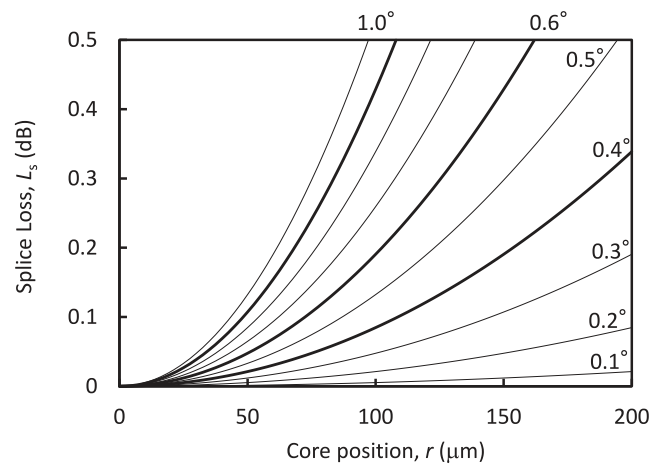
Fig. 3. Calculated splice loss as a function of core position for various angle alignment errors.

where $2w_1$ and $2w_2$ are the mode field diameters of the spliced fibers and d is the offset of the core centers of the spliced fibers. If fibers whose cores are positioned at r from the center of a cladding are aligned with the angle error θ, d is given by

$$d = 2r \sin (\theta/2). \quad (5)$$

Fig. 3 shows the estimated splice losses as a function of core position for different angle alignment errors according to (4) and (5). Both $2w_1$ and $2w_2$ are 10 μm. As the distance from the center of the cladding increase, excess splice loss due to errors in angle alignment is increased. Reference [21] reported that the averaged, maximum, and minimum angle alignment error was 0.6°, 0.9°, and 0.4° for a commercially available fusion splicer that aligns cores with fiber-rotation and end-view functions [22]. A large r requires a small angle alignment error for realizing a small splice loss. The r will be limited to approximately 75 μm to achieve an averaged splice loss < 0.1 dB for the current fusion splicer. The limit may be relaxed owing to the improvement of alignment accuracy and the enlargement of the mode field diameter of the spliced fiber. For fibers with $2w_1 = 2w_2 = 12\ \mu$m, whose effective area is larger than 110 μm^2, the r for achieving the splice loss < 0.1 dB is increased to approximately 85 μm. However, the increased effective area is not preferable
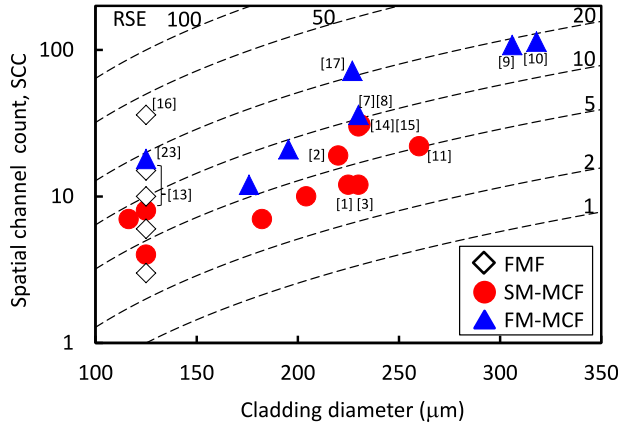
Fig. 4. SCC as a function of cladding diameter for FMFs (open lozenge symbols), SM-MCFs (red solid circle symbols), and FM-MCFs (Blue triangle symbols). Contour lines are RSE.

Fig. 5. SCC as a function of 100-km worst XT at 1550 nm for MCFs presented so far.

for reducing XT. Accordingly, the splice ability may become a limiting factor for the D_c.

Fig. 4 shows the SCC of recently proposed MCFs and FMFs as a function of cladding diameter. The contour lines indicate the RSE.

The cladding diameter of almost all FMFs presented so far was 125 μm. The SCC, i.e., the mode count for an FMF with 125-μm cladding diameter, and RSE reached the value of 36 [16], [27]. However, the DMD becomes considerably sensitive against structural parameter fluctuations that depend on the increase in SCC [16], [27]. The required DMD level for realistic signal processing is a limiting factor for the SCC of the FMFs.

At this time, the maximum SCC of SM-MCFs is over 30. An MCF with 30 cores employed a heterogeneous core structure to realize high core count and low XT simultaneously [14]. The fiber contained 30 cores with A_{eff} of 80 μm^2 in a 230-μm cladding, and it marked an RSE of 8.9. An MCF with 31 cores employed QSM design [15]. The RSE of the 31-core fiber was 9.1, which is the highest value of the SM-MCF.

Another approach for improving spatial multiplicity is using the FM-MCF. The FM-MCFs investigated so far can be categorized into three groups. The first group includes a fiber with a cladding diameter of 125 μm [23]. The fiber exhibited an SCC of 18 and RSE of 18. The second group focuses on improving the SCC [9], [10]. Two fibers recorded an SCC larger than 100 and RSE of approximately 18. However, their cladding diameter exceeded 300 μm. The validity of such large cladding diameters in terms of mechanical reliability and splicing needs to be further analyzed. The last group aims to maximize the SCC and RSE under a moderate cladding diameter smaller than 250 μm. A three-mode (two LP modes) 12-core fiber with a cladding diameter of 230 μm exhibited an SCC of 36 and RSE of 10.64. Another example is a six-mode (four LP modes) 12-core fiber with a cladding diameter of 227 μm. This fiber exhibited an SCC of 72 and RSE of 21.83, which is the highest RSE for MCFs presented so far.

C. SCC Versus Core-to-Core XT

XT is an important parameter to compare the performance of MCFs. XT limits the transmission distance, transmission
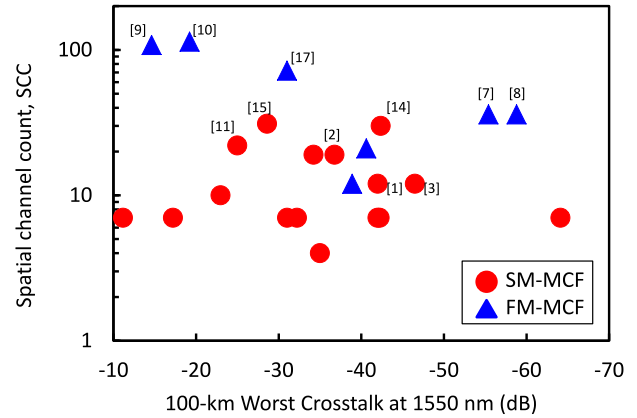
capacity, and modulation format [24]. Fig. 5 indicates the relationship between SCC and XT for the presented MCFs. We employed the XT between the highest order modes as the XT of FM-MCFs because the XT between the highest order modes is larger than the XT among other combination of modes [25]. MCFs with low XT < −40 dB/ 100 km have contributed to achieve some remarkable transmission: a 12-core fiber with ring structure for 1 Pbit/s/fiber transmission with 32QAM [1], a 12-core fiber with a dual-ring structure for 1 Ebit/s km transmission with 16QAM [3], a 7-core fiber with hexagonal closed pack structure for 1 Ebit/s km transmission over transoceanic distance [4], and an FM-MCF with a square lattice structure for dense SDM of 36 SCC over 527 km [8].

Recently proposed SM-MCFs with SCC of 30 and more [14], [15] and FM-MCF with SCC of 72 [17] showed XT of about −30 dB/ 100 km. These fibers will contribute to transmission with large capacity or high-order modulation.

The combination of SCC and XT is affected by A_{eff} and the cladding diameter [26]. With regard to a long-haul system, an MCF with large A_{eff} and small XT is required. This requirement limits the SCC. The possible SCC will be determined by the requirement on A_{eff} and XT from the transmission system.

D. SCC Versus DMD

In the case of FMFs and FM-MCFs, DMD, which is the time difference between the fastest mode and the slowest mode in a core, is a very important parameter because a large DMD requires heavy signal processing for recovering mode-coupled signals. Fig. 6 shows the relationship between the maximum |DMD| and SCC of FMFs and FM-MCFs. References [16] and [25] suggest that DMD control becomes very difficult as the mode count become large. The |DMD| of FMFs whose mode count is larger than 10 ranged at a few hundred ps/km. A multistep profile and a graded index profile are useful to reduce |DMD| and control DMD characteristics [16], [27], [28]. The DMD characteristics of fabricated fibers also depend on the fabrication process of the fiber. The process such as modified chemical vapor deposition (MCVD) is preferable to control index profiles precisely.
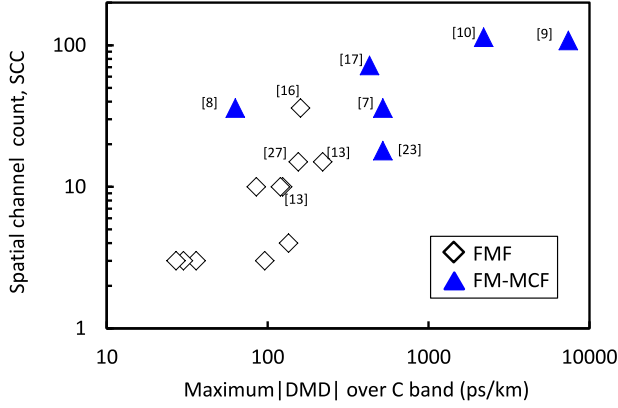
Fig. 6. SCC as a function of measured maximum DMD over the C band. Some data were the |DMD| at 1550 nm.

Fig. 8. Schematic of the dependence of bending radius R on XT.
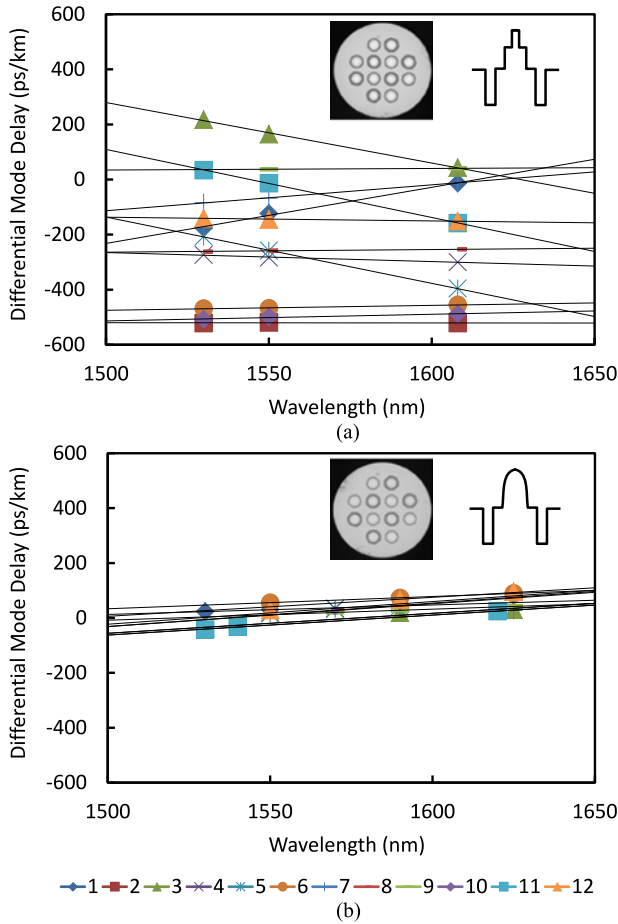

Fig. 7. Measured wavelength dependence of the DMD for two kinds of FM-MCFs with 36 spatial channels [18], [29]: (a) A fiber with a multi-step index profile [7]. (b) A fiber with a graded index profile [8]. Symbols indicate the measured DMD. Lines indicate a linear approximation of the measured data.

FM-MCFs require suppressing |DMD| for all cores within a certain range. The |DMD| of the FM-MCFs with SCC larger than 100 was greater than 1000 ps/km [9], [10]. The |DMD| over the C band of the FM-MCFs with SCC of 36 was drastically reduced from 530 to 63 ps/km as shown in Fig. 7 [18], [29]. The fiber in Fig. 7(a) had cores with a multistep profile and was fabricated by the vapor-phase axial deposition method. The fiber in Fig. 7(b) had cores with a graded-index profile and

was fabricated by the MCVD method. The combination of the change of index profile and fabrication process realized DMD reduction. The reduction of |DMD| enables the lengthening of the transmission distance from 40.4 [7] to 527 km [8]. The FM-MCF with SCC of 72, which involves 12 cores with six modes (four LP modes), successfully controlled |DMD| under less than 430 ps/km for all cores owing to a graded index profile [17]. We need to select the combination of CC and MC with the tradeoff relationship between SCC and DMD in mind.

III. SINGLE-MODE 30-CORE FIBER WITH HETEROGENEOUS CORE DESIGN

A. Fiber Design

Heterogeneous core design means that the effective indices (n_{eff}s) are different for all adjacent cores [30]. If the n_{eff}s of the adjacent cores are different, the XT between the cores drastically changes at a certain bending radius (R_{pk}) [31], as shown in Fig. 8. R_{pk} is given by

$$R_{pk} = \frac{n_{eff}}{\Delta n_{eff}} \Lambda, \qquad (6)$$

where n_{eff} is the effective index of a propagation mode, Δn_{eff} is the effective index difference between cores, and Λ is the core pitch. If the bending radius R is less than R_{pk}, XT is given by the following equation [31].

$$XT = \frac{2\kappa^2 R}{\beta \Lambda} L \qquad (7)$$

where k is the coupling coefficient, β is the propagation constant, and L is the length of a fiber. In this case, XT varies with bending radius R. Accordingly, we can call this region the R-dominant region. In contrast, if the bending radius R is larger than R_{pk}, XT is given by the following equation [32]:

$$XT = \frac{2\kappa^2}{\Delta \beta^2 d} L \qquad (8)$$

where d is the correlation length. In this case, the XT of the region varies with d and we consider this region d-dominant. The XT over the d-dominant region is smaller than that over the R-dominant region. By setting the R_{pk} value below the effective bending diameter in cables, we can reduce the XT of an MCF and maximize the number of cores within a limited range of

Fig. 9. A heterogeneous SM-MCFs with 30 cores [14], [28]: (a) A schematic of the fiber structure. (b) A cross-sectional view of a fabricated fiber. (c) Index profiles of the cores.
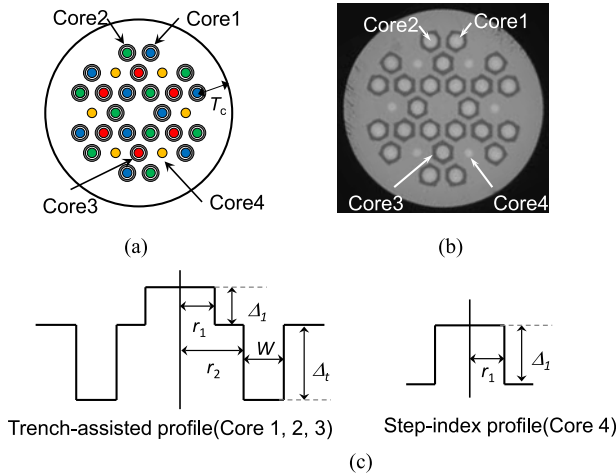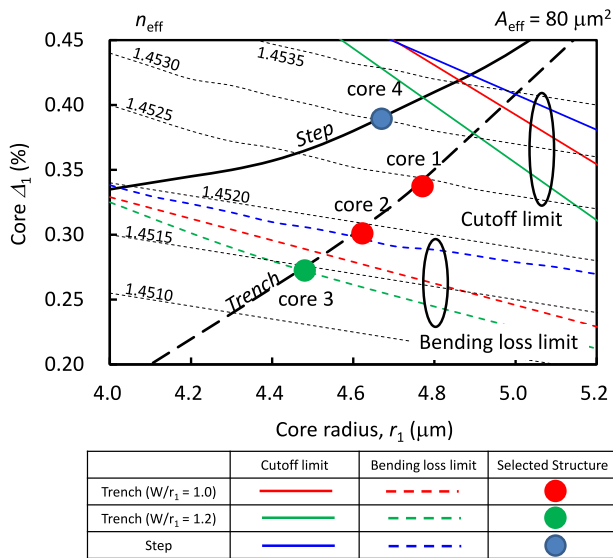

Fig. 10. Relationship between the core parameters and effective indices in trench-assisted and step-index cores for a 30-core fiber [14], [18], [29].

TABLE I
SIMULATION RESULTS FOR A HETEROGENEOUS 30-CORE FIBER

Core Type	r_1 [μm]	Δ_1 [%]	r_2/r_1	W/r_1	$A_{\rm eff}$ [2] [μm^2]
Core 1[1]	4.76	0.338	1.7	1.0	80.2
Core 2[1]	4.62	0.305	1.7	1.0	80.3
Core 3[1]	4.47	0.273	1.7	1.2	80.2
Core 4	4.68	0.388	–	–	80.0

Combination	$\Delta n_{\rm eff}$ [2]	$R_{\rm pk}$ [3] [mm]
Core 1–2	0.00051	86
Core 1–3	0.00100	44
Core 1–4	0.00063	69
Core 2–3	0.00050	88
Core 2–4	0.00113	38
Core 3–4	0.00163	27

[1] $\Delta_{\rm t} = -0.7\%$.
[2] Calculated wavelength $= 1550$ nm.
[3] Core pitch, $\Lambda = 30$ μm.

on a hexagonal closed-pack structure with 37 cores. The six outermost cores were removed to reduce the cladding diameter. The central core was also removed because wavelength lengthening of the core due to the trench-assisted structure was unavoidable [35]. Four kinds of cores were used to produce a heterogeneous relation for all adjacent cores under the limitation of using the same $A_{\rm eff}$ for all cores. Core 1, 2, and 3 employed a trench-assisted structure to reduce the XT. Core 4 had no trench layer to avoid the cutoff wavelength lengthening of the inner cores. Table I summarizes the core parameters derived from Fig. 10. The $\Delta n_{\rm eff}$s were larger than 0.0005 for all combinations. The $\Delta n_{\rm eff}$s ensured that the $R_{\rm pk}$ was less than 100 mm for a Λ of 30 μm. If we set the cladding diameter at 230 μm, the T_c will be 35.6 μm, which is sufficient for reducing the excess loss due to a high-index coating [35].

B. Characteristics of a Fabricated Fiber

Fig. 9(b) shows a cross sectional view of a fabricated 30-core fiber. We fabricated 9.6-km fiber with a D_c of 228 μm and Λ of 29.7 μm using the stack and draw method. The averaged attenuation and averaged $A_{\rm eff}$ at 1550 nm were 0.50 dB/km and 77.3 μm^2, respectively. The high attenuation was caused by problems in the process during stacking. The cable cutoff wavelengths were less than 1.57 μm, which was larger than the designed value of less than 1.53 μm. The lengthening of the cutoff wavelength originated from the profile difference between the simulation and fabricated fiber. Fig. 11 shows the measured XT of a 9.6-km fiber wound on a spool with a diameter of 310 mm. We evaluated the XT using statistical measurements by sweeping the wavelength [35]. A single-core fiber with a trench structure was used as the incident and receiving fiber to improve the dynamic range of XT [36], which was about 80 dB for our set-up. The measured XT for the 9.6-km fiber was, on average, less than –55 dB for all kinds of combinations.

We also measured the XT for a 22-m fiber to confirm the $R_{\rm pk}$ of the fabricated fiber, as shown in Fig. 12. The solid symbols

cladding diameters. However, the different $n_{\rm eff}$ design has the tendency to produce different $A_{\rm eff}$ values, which is not desirable for realizing homogeneity of transmission characteristics and low splice loss.

The same $A_{\rm eff}$ for all the cores with heterogeneous $n_{\rm eff}$ is achievable through the careful selection of core parameters such as the core radius (r) and relative index difference (Δ) [33], [34]. However, the same $A_{\rm eff}$ with heterogeneous $n_{\rm eff}$ design limits the range of core parameters to ensure the single-mode condition and reduce the bending loss of the fundamental mode [33].

Fig. 9 shows the schematic structure and cross-sectional view of a fabricated heterogeneous SM-MCF with 30 cores. T_c is the outer cladding thickness, which is the distance between the center of an outermost core and the edge of a cladding. Fig. 10 shows the simulation results for fiber core design [14], [18], [29]. The lines of the cutoff limit and bending loss limit were calculated for each structure. The lines of $n_{\rm eff}$ were drawn for the trench-assisted structure. The structure of the fiber was based
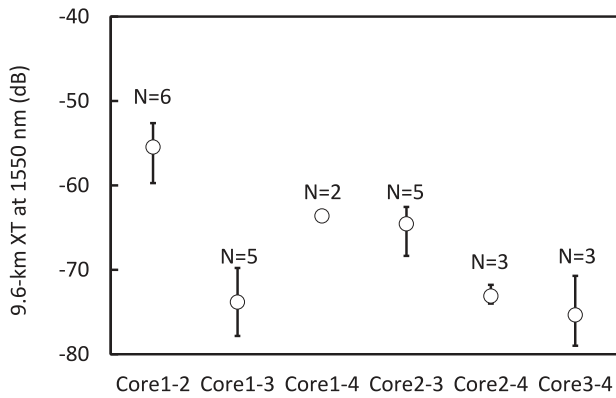
Fig. 11. Measured XT at 1550 nm for a 9.6-km fiber. Core *i-j* means the XT between core *i* and core *j*. *N* indicates the number of measurements for core i-j.

indicate the measured XT and the solid lines show the calculated XT for different d values. We measured the XT of the freely coiled fiber at $R = 140, 70$, and 35 mm. The measurement limit for XT in our system was about –70 dB. The results indicate that, as designed, the R_{pk} of the fabricated fiber was around 100 mm. The measured XTs for bending radii $< R_{pk}$ agree well with the simulation results. However, the measured XTs for bending radii $> R_{pk}$ were smaller than the XT estimated with $d = 50$ mm, which was reported in [34]. We were not able to evaluate d from the measured results because the results were smaller than the measurement limit. Further study is required for XT simulation of a heterogeneous MCF.

IV. SINGLE-MODE 31-CORE FIBER WITH QSM CORE DESIGN

As demonstrated in the previous section, a heterogeneous core is quite effective for reducing XT. However, precise process control of the core structure is required for preparing heterogeneous cores. In this section, we demonstrate a high-core-count MCF with homogeneous structure.

A. Fiber Design

As shown in Fig. 5, the FM-MCF concept is helpful for realizing large SCC and small XT simultaneously. However, heavy signal processing is required to recover the distorted signal due to mode coupling. QSM transmission is a technique that uses only the fundamental mode of an FMF. We are able to get the freedom for fiber design by lengthening the cutoff wavelength with QSM design. In the case of QSM design for a conventional single-core fiber, we used the freedom to enlarge the A_{eff}. QSM transmission experiments over the FMFs have been successfully demonstrated [37]. The advantage of QSM transmission is the reduction of the nonlinearity of transmission lines owing to the enlarged A_{eff} of the fundamental mode of FMFs. However, in the case of MCF design, we used the freedom to strengthen the confinement of the fundamental mode instead of A_{eff} enlargement. An advantage of applying QSM transmission to MCF designs is the XT reduction owing to the high confinement of the LP_{01} mode in a few-mode core. The suppression of XT enables a dense core arrangement within a limited range of cladding diameters. It has been reported that the undesired
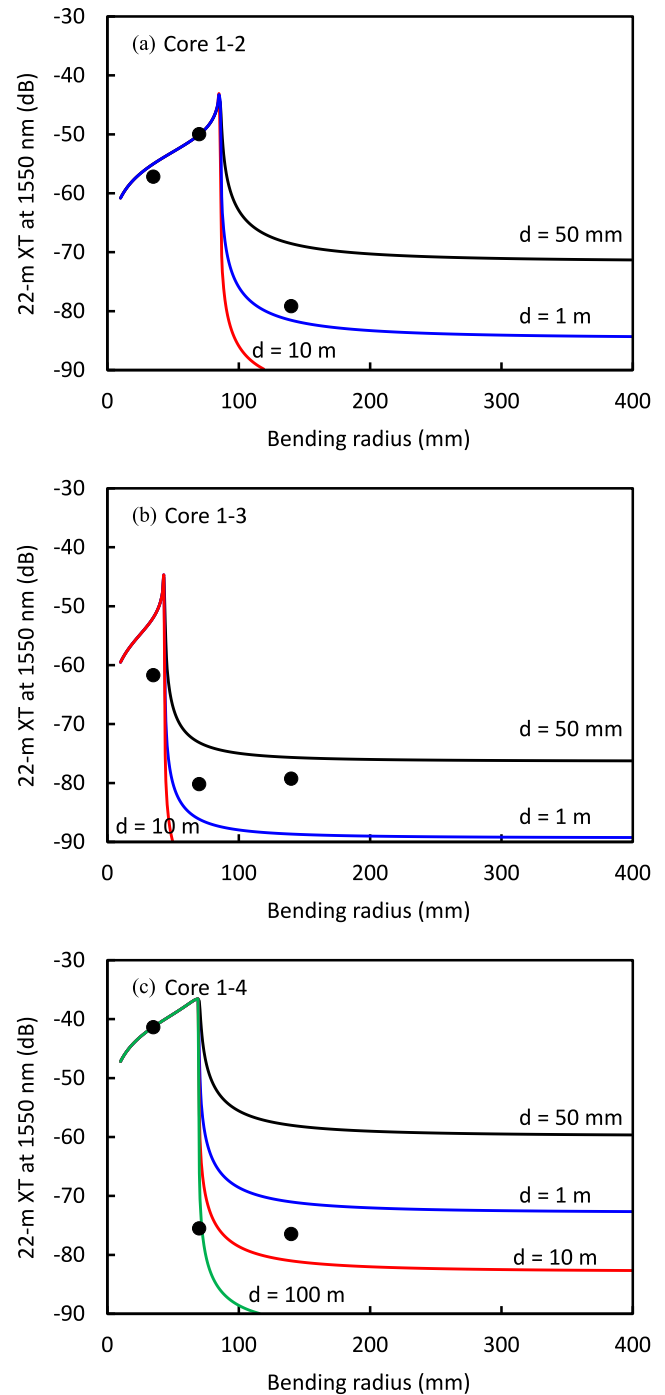
Fig. 12. Measured and simulated XT at 1550 nm for a 22-m fiber. Core *i-j* means the XT between core *i* and core *j*. *N* indicates the number of measurements for core *i-j*. The solid symbols are measured results. The lines indicate the simulated XT with a correlation length of 50 mm.

remaining LP_{11} mode, which is generated during signal propagation through fibers and at splice points, deteriorates the quality of LP_{01}-mode signals [37], [38]. The intentional elimination of the LP_{11} mode is helpful in reducing signal deterioration.

In the case of the MCFs, the propagating power in the outermost cores can be absorbed into a coating with a low outer cladding thickness (T_c). In general, the field size of an LP_{11} mode is far larger than that of an LP_{01} mode. Accordingly, an

TABLE II
CORE PARAMETERS FOR SIMULATION

ID	Δ [%]	r_1 [μm]	r_2/r_1	W/r_1
Design 1	0.45	86	1.7	0.8
Design 2	0.45	38	1.7	0.9
Design 3	0.45	27	1.7	1.0
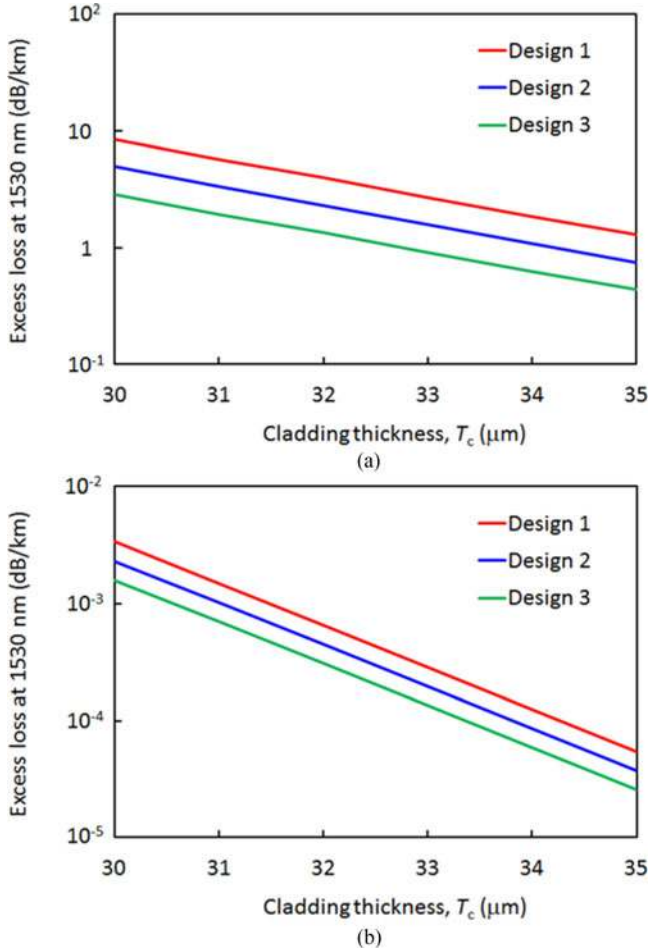
Fig. 13. Calculated excessive losses as a function of outer cladding thickness (T_c) for the cores shown in Table II, (a) LP_{11} mode, (b) LP_{01} mode.

optimized T_c helps realize the coexistence of the large excessive loss of an LP_{11} mode and the negligible excessive loss of an LP_{01} mode in the outermost cores. The direct coating absorption of the inner cores is far smaller than that of the outermost cores. However, the power of an LP_{11} mode is expected to leak to a coating through the XT from the inner cores to the outer cores.

We designed a QSM MCF using the above concepts. The fiber contains 31 trench-assisted homogeneous cores in a hexagonal close-packed structure with a cladding diameter of 230 μm [15]. The A_{eff} at 1550 nm was set as 80 μm^2, which is the same as that of a conventional SMF. A trench-assisted structure, which is shown in Fig. 9(c), was used for all cores. We optimized the core parameters and T_c by simulation. Table II summarizes the core parameters used in the simulation and $\Delta_t = -0.7\%$. Fig. 13 shows the calculated excessive loss of the LP_{11} mode at 1530 nm
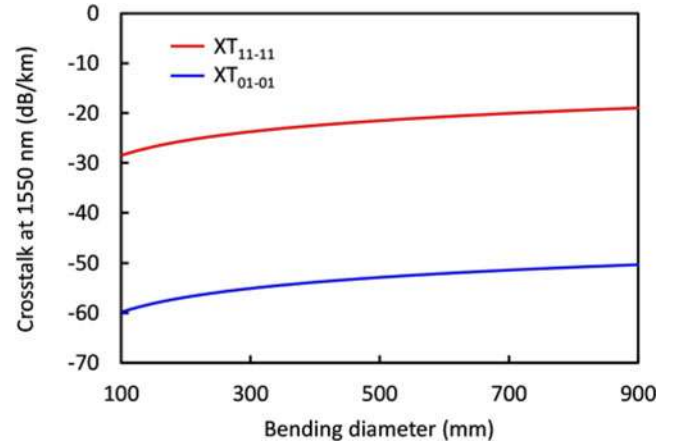
Fig. 14. Calculated core-to-core XT for the same mode in cores at 1550 nm as a function of bending diameter.
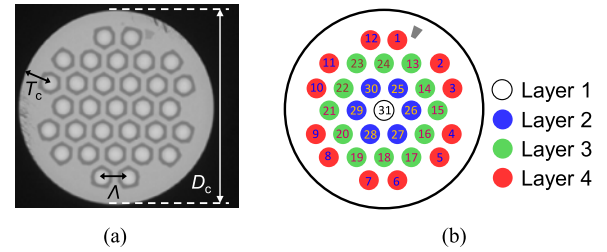
Fig. 15. A fabricated QSM 31-core fiber: (a) A cross-sectional view. (b) The definition of the layer and core numbers.

and the LP_{01} mode at 1625 nm due to absorption into the coating as a function of T_c with a bending diameter of 280 mm. We employed an LP_{01}-excessive-loss of 0.001 dB/km as a reference. Design 1 requires a relatively large T_c to realize the employed LP_{01}-excessive-loss. Design 3 shows a small LP_{11}-excessive-loss for an LP_{01}-excessive-loss of 0.001 dB/km. Design 2 is a well-balanced design that achieves an LP_{11}-excessive-loss greater than 3 dB/km and an LP_{01}-excessive-loss smaller than 0.001 dB/km at a T_c of about 31 μm. Fig. 14 shows the calculated core-to-core XT at 1550 nm between the LP_{11} modes (XT_{11-11}) and between the LP_{01} modes (XT_{01-01}) as a function of the bending diameter for a core pitch (Λ) of 32 μm. XT_{01-01} less than –46 dB/km, which leads to XT of –19 dB after 500-km transmission, is satisfied under a bending diameter of several hundred millimeters. The large XT enables QPSK transmission over 500 km with a Q-penalty of 0.5 dB [24], [39]. XT_{11-11} exceeds XT_{01-01} by more than 30 dB. This is helpful for transferring the power of the LP_{11} mode in the inner cores to the outermost cores, where the power of the LP_{11} mode is expected to be absorbed into the coating.

B. Characteristics of the Fabricated Fiber

We fabricated a homogeneous QSM 31-core fiber based on design 2 [15]. Fig. 15 shows a cross section and the layer/core assignments of the fiber. Λ, T_c, and D_c of the fabricated fiber was 31.6, 31.5, and 231 μm, respectively. Table III summarizes the averaged optical characteristics of some cores in each layer.

TABLE III
MEASURED CHARACTERISTICS OF A FABRICATED FIBER

	Layer 1	Layer 2	Layer 3	Layer 4
A_{eff}* [μm^2]	75.0	75.0	74.4	75.3
λ_{cc} [μm]	2.04	1.95	1.89	1.68

A_{eff}^* of the fundamental mode measured at 1550 nm.
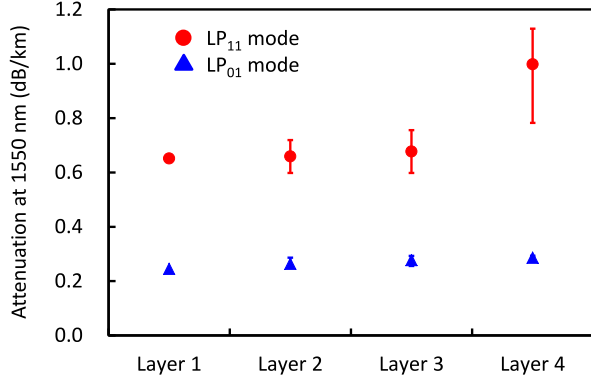

Fig. 16. Measured attenuation of the LP_{01} and LP_{11} modes at 1550 nm. The red circles and blue triangle symbols are the average attenuation of each layer. The bars indicate the maximum and minimum value of each layer.

The cable cutoff wavelengths (λ_{cc}s) of the inner cores were far longer than those of the outer cores owing to the existence of outer trench-assisted cores [35].

Fig. 16 shows the measured attenuation of each mode. The attenuation of the LP_{11} mode, particularly in layer 4, was far larger than that of the LP_{01} mode. This indicates that the power of the LP_{11} mode was conspicuously absorbed into the coating. The measured attenuation (α_{total}) of a core is given by the following equation:

$$\alpha_{\mathrm{total}} = \alpha_{\mathrm{pro}} + \alpha_{\mathrm{XT}} + \alpha_{\mathrm{ex}}, \qquad (9)$$

where α_{pro} is the loss without the influence of absorption and XT, α_{XT} is the loss due to XT, and α_{ex} is the excessive loss due to the coating. α_{pro} was assumed as the attenuation of the LP_{01} mode, because the attenuation of the LP_{11} mode with sufficiently thick T_c and low XT is almost equal to that of the LP_{01} mode [40]. The α_{ex} of core 8 was estimated to be 0.6 dB/km, which is smaller than the calculation shown in Fig. 13(a).

Fig. 17 shows the measured XT_{11-11} and XT_{01-01} at 1550 nm. The fiber length was 11 km, and the bending diameter was 310 mm. XT_{01-01} was derived from linear extrapolation of the wavelength dependency of the measured XT over the single-mode region. The averaged XT_{01-01} and XT_{11-11} were –38.4 and –5.5 dB, respectively. The measured XT_{01-01} and XT_{11-11} were larger than the simulated values of –41.9 and –10.5 dB, respectively. These discrepancies arose from the difference between the ideal step profile used in the simulations and the actual profile.

Fig. 18 shows the measured near field pattern (NFP) of the 31-core fiber to confirm LP_{11}-mode power transition from the central core (core 31) to the outer cores. Only core 31 was excited by the LP_{11} mode. The LP_{11}-mode power in core 31
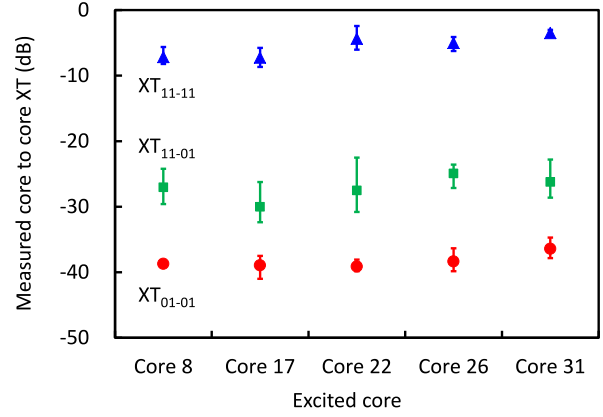
Fig. 17. Measured core-to-core XT at 1550 nm between LP_{11} modes (XT_{11-11}, blue triangle symbols), between LP_{01} modes (XT_{01-01}, red circle symbols), and between LP_{11} and LP_{01} (XT_{11-01}, green square symbols). The bars indicate the maximum and minimum values among cores adjacent to the excited core.
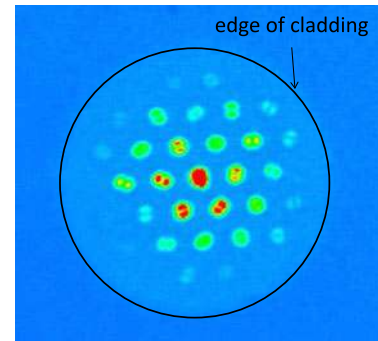
Fig. 18. Measured NFP of the fabricated 31-core fiber. Only the central core (core 31) was excited by the LP_{11} mode.
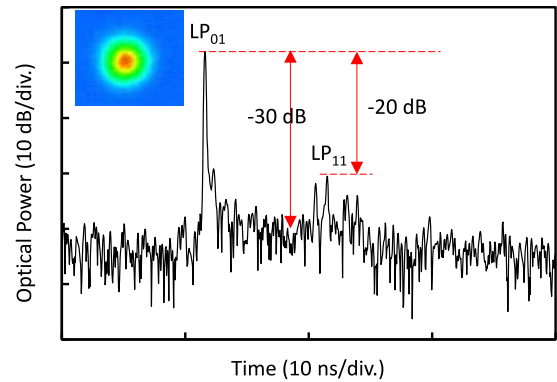
Fig. 19. Measured impulse response and NFP from a core in layer 2 of the 11-km fiber with an FI device. The inset shows a NFP after 11-km transmission.

was moved to neighboring cores owing to the large XT between the LP_{11} modes.

We confirmed LP_{11} suppression after 11-km propagation. Fig. 19 shows the impulse-response signal of a core in layer 2 after 11-km transmission. An LP_{01}-mode pulse was introduced to the fiber through a waveguide-type fan-in (FI) device [41]. The inter-mode XT through the fiber was smaller than –30 dB. The LP_{11} mode generated at a connection point of the FI and fiber was observed at the time predicted from the DMD of the
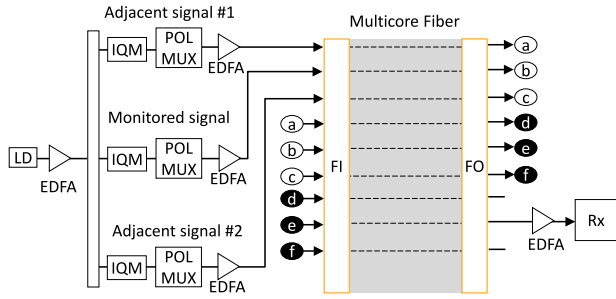
Fig. 20. Experimental set up for evaluating the transmission characteristics of MCFs.
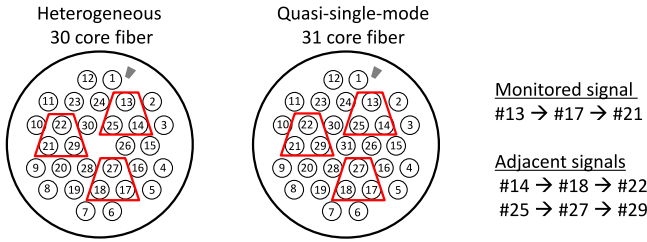
Fig. 21. Signal assignment for the transmission experiment on the 30-core and 31-core fibers.

LP_{11} mode to the LP_{01} mode. The power was –20 dB less than that of the LP_{01} mode. We have concluded that the power of the received LP_{11} mode was sufficiently small after 11-km propagation, which is also supported by a NFP from another end, as shown in the inset of Fig. 18.

V. TRANSMISSION EXPERIMENTS

We evaluated and compared the transmission characteristics of the heterogeneous 30-core fiber and the QSM 31-core fiber.

A. Measurement Setup

Fig. 20 shows the schematics of our measurement setup. Thee modulators were prepared. We used the signal from a modulator for monitoring the Q value. The signals from other modulators were used as dummy signals to adjacent cores to evaluate the degradation of the Q value due to XT from the adjacent cores. We prepared two kinds of modulators; polarization multiplexed QPSK and polarization multiplexed 16 QAM. The baud rate for both formats was 11.5 Gbaud. The signals were circulated three times through fan-in/fan-out (FI/FO) devices. The Q value of the monitored signal after three-span propagation was monitored. The total transmission distance was 28.8 km (9.6 km × 3) for the 30-core fiber and 33 km (11 km × 3) for the 31-core fiber. Fig. 21 shows signal assignment for the 30-core and 31-core fibers.

Fig. 22 shows XT characteristics of the fibers with FI/FO devices. We employed FI/FO devices with a wave guide structure [41]. Table IV summarizes XT and attenuation at 1550 nm of three spans.

The back-to-back Q value of the measurement setup was 9.0 dB for QPSK transmission and 10.2 dB for 16QAM transmission.
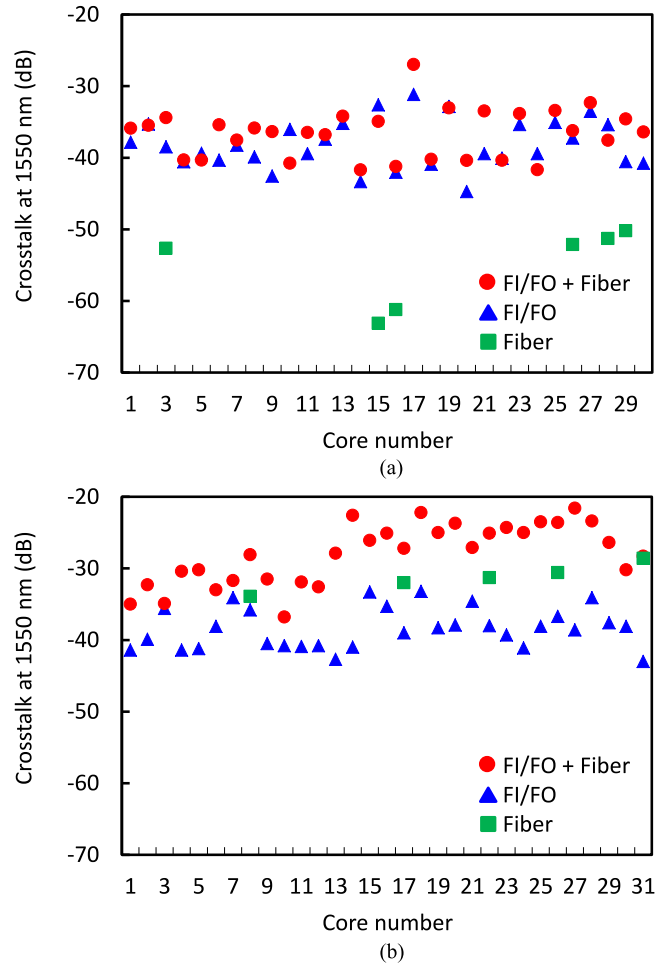
Fig. 22. Measured XT characteristics of the fiber, FI/FO, and FI/FO + Fiber: (a) Heterogeneous 30-core fiber. (b) QSM 31-core fiber.

TABLE IV
THREE SPAN CHARACTERISTICS OF HIGH-CORE-COUNT MCF WITH FI/FOS

	Heterogeneous 30-core fiber	QSM 31-core fiber
XT [dB]	−26.9	−16.6
Attenuation [dB]	32.5	20.1

B. Transmission Characteristics

In the case of QPSK transmission over the heterogeneous 30-core fiber, a small Q penalty of 0.2 dB was observed for both one-core transmission and three-core transmission. The Q penalty of 16 QAM was slightly larger than that of QPSK. However, Q penalty was kept small for both 0.4 dB one-core transmission and 0.7 dB three-core transmission.

In contrast, degradation was observed for the Q value over the QSM 31-core fiber. The Q penalty of one-core transmission with QPSK was 0.4 dB. However, the Q penalty became 1.4 dB for three-core transmission. In the case of 16QAM, the Q penalty was 1.7 dB even for one-core transmission. The Q penalty for three-core transmission was 4.1 dB.
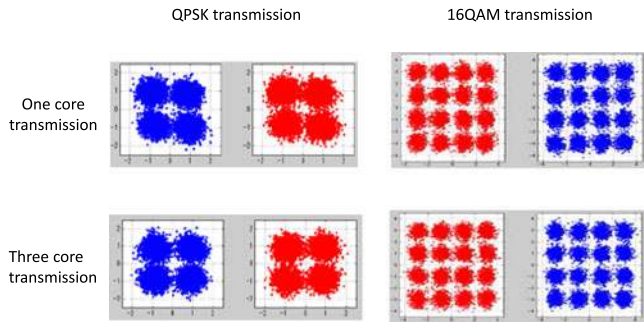
Fig. 23. Constellation map over a heterogeneous 30-core fiber with QPSK and 16 QAM for each polarization. Additional ASE noise was imposed to be visible the change of the constellation map.
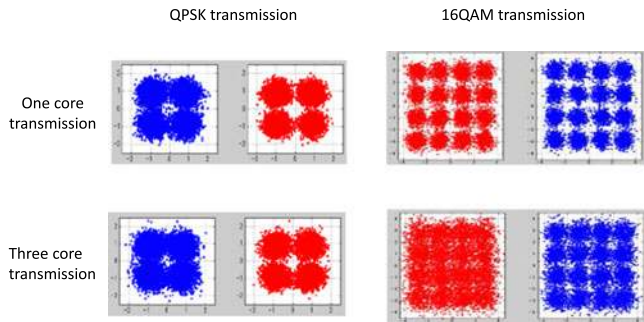
Fig. 24. Constellation map over a QSM 31-core fiber with QPSK and 16 QAM for each polarization. Additional ASE noise was imposed to be visible the change of the constellation map.
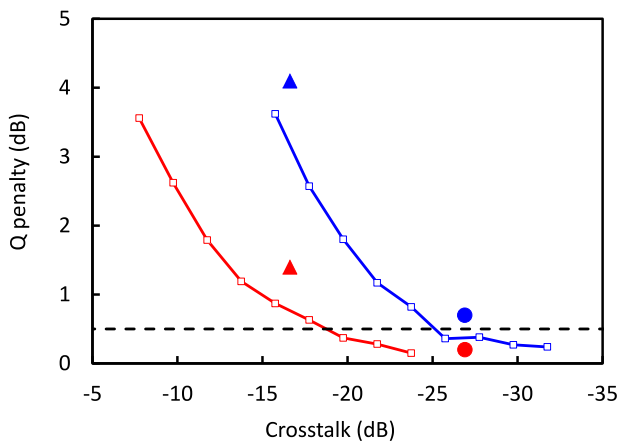
	Heterogeneous 30-core fiber	Quasi-Single-mode 31-core fiber	Homogeneous 12-core fiber [37]
QPSK	●	▲	□—
16QAM	●	▲	□—

Fig. 25. Measured *Q* penalty as a function of XT. Circle symbols and triangle symbols indicate the measured *Q* penalty for 30-core and 31-core fiber. Square symbols indicate measured *Q* penalty of our previous experiment on 12-core fiber [39].

Figs. 23 and 24 show the measured constellation maps over the heterogeneous 30-core fiber and the QSM 31-core fiber, respectively. The ASE noise was added to make the *Q*-degradation tendency for fibers and modulation formats understandable. The

constellation maps demonstrated the same tendency with the measured *Q* value.

Fig. 25 shows the measured *Q* penalty as a function of XT for different modulation formats. Circle and triangle symbols indicate the measured *Q* penalty for 30- and 31-core fibers. Square symbols indicate measured *Q* penalty for 12-core fiber [37]. For the 12-core fiber, the required XT is less than −18 dB for QPSK and less than −25 dB for 16 QAM when the allowable *Q* penalty is 0.5 dB. The measured *Q* values of the heterogeneous 30-core fiber are close to those of the 12-core fiber. However, an additional penalty was observed for the measured *Q* values of the QSM 31-core fiber. Because the additional penalty will originate from the mode coupling during propagation and XT between cores, we need to suppress the higher-order mode propagation.

VI. CONCLUSION

The development trend of MCFs for dense spatial division multiplexing was reviewed. Many kinds of MCFs have been proposed to overcome the tradeoff relationship among the SCC, cladding diameter, XT, and DMD.

The design concept and fabrication results of SM-MCFs with an SCC of larger than 30 was presented. A 30-core fiber with a heterogeneous core was realized with a low XT of −55 dB and length of 9.6 km and a low *Q* penalty for QPSK and 16 QAM. A 31-core fiber with the QSM recorded the highest SCC as an SM-MCF. The *Q* penalty due to the XT was observed during the transmission experiment on the 31-core fiber. The characteristics will improve by suppressing the higher-order mode propagation.

REFERENCES

[1] H. Takara, A. Sano, T. Kobayashi, H. Kubota, H. Kawakami, A. Matsuura, Y. Miyamoto, Y. Abe, H. Ono, K. Shikama, Y. Goto, K. Tsujikawa, Y. Sasaki, I. Ishida, K. Takenaga, S. Matsuo, K. Saitoh, M. Koshiba, and T. Morioka, "1.01-Pb/s (12 SDM/222 WDM/456 Gb/s) crosstalk-managed transmission with 91.4-b/s/Hz aggregate spectral efficiency," presented at the Eur. Conf. Exhib. Optical Communication, Amsterdam, The Netherlands, 2012, Paper Th.3.C.1.

[2] J. Sakaguchi, W. Klaus, B. J. Puttnam, J. M. D. Mendinueta, Y. Awaji, N. Wada, Y. Tsuchida, K. Maeda, M. Tadakuma, K. Imamura, R. Sugizaki, T. Kobayashi, Y. Tottori, M. Watanabe, and R. V. Jensenexa, "19-core MCF transmission system using EDFA with shared core pumping coupled via free-space optics," *Opt. Exp.*, vol. 22, no. 1, pp. 90–95, Jan. 2014.

[3] T. Kobayashi, H. Takara, A. Sano, T. Mizuno, H. Kawakami, Y. Miyamoto, K. Hiraga, Y. Abe, H. Ono, M. Wada, Y. Sasaki, I. Ishida, K. Takenaga, S. Matsuo, K. Saitoh, M. Yamada, H. Masuda, and T. Morioka, "2 × 344 Tb/s propagation-direction interleaved transmission over 1500-km MCF enhanced by multicarrier full electric-field digital back-propagation," presented at the Eur. Conf. Exhib. Optical Communication, London, U.K., 2013, Paper PD3.E.4.

[4] K. Igarashi, T. Tsuritani, I. Morita, Y. Tsuchida, K. Maeda, M. Tadakuma, T. Saito, K. Watanabe, K. Imamura, R. Sugizaki, and M. Suzuki, "Super-Nyquist-WDM transmission over 7,326-km Seven-core Fiber with Capacity-distance Product of 103 Exabit/s·km," *Opt. Exp.*, vol. 22, no. 2, pp. 1220–1228, Jan. 2014.

[5] V. A. J. M. Sleiffer, Y. Jung, V. Veljanovski, R. G. H. van Uden, M. Kuschnerov, Q. Kang, L. Grüner-Nielsen, Y. Sun, D. J. Richardson, S. Alam, F. Plletti, J. K. Safu, A. Dhar, H. Chen, B. Inan, A. M. J. Koonen, B. Corbett, R. Winfield, A. D. Ellis, and H. de Waardt, "73.7 Tb/s(96×3×256-Gb/s) mode-division-multiplexed DP-16QAM transmission with inline MM-EDFA," presented at the Eur. Conf. Exhib. Optical Communication, Amsterdam, 2012, Paper Th.3.C.4.

[6] N. K. Fontaine, R. Ryf, H. Chen, A. V. Benitez, J. E. A. Lopez, R. A. Correa, B. Guan, B. Ercan, R. P. Scott, S. J. B. Yoo, L. Grüner-Nielsen, Y. Sun, and R. J. Lingle, "30×30 MIMO transmission over 15 spatial

modes," presented at the Optical Fiber Communication Conf., Los Angeles, CA, USA, 2015, Paper Th5C.1.

[7] T. Mizuno, T. Kobayashi, H. Takara, A. Sano, H. Kawakami, T. Nakagawa, Y. Miyamoto, Y. Abe, T. Goh, M. Oguma, T. Sakamoto, Y. Sasaki, I. Ishida, K. Takenaga, S. Matsuo, K. Saitoh, and T. Morioka, "12-core x 3-mode dense space division multiplexed transmission over 40 km employing multi-carrier signals with parallel MIMO equalization," presented at the Optical Fiber Communication Conf., San Francisco, CA, USA, 2014, Paper Th5B.2.

[8] K. Shibahara, T. Mizuno, H. Takara, A. Sano, H. Kawakami, D. Lee, Y. Miyamoto, H. Ono, M. Oguma, Y. Abe, K. Kobayashi, T. Matsui, R. Fukumoto, Y. Amma, T. Hosokawa, S. Matsuo, K. Saito, H. Nasu, and T. Morioka, "Dense SDM (12-core x 3-mode) transmission over 527 km with 33.2-ns mode-dispersion employing low-complexity parallel MIMO frequency-domain equalization," presented at the Optical Fiber Communication Conf., Los Angeles, CA, USA, 2015, Paper Th5C.3.

[9] J. Sakaguchi, W. Klaus, J.-M. D. Mendinueta, B. J. Puttnam, R. S. Luis, Y. Awaji, N. Wada, T. Hayashi, T. Nakanishi, T. Watanabe, Y. Kokubun, T. Takahata, and T. Kobayashi, "Realizing a 36-Core, 3-mode fiber with 108 spatial channels," presented at the Optical Fiber Communication Conf., Los Angeles, CA, USA, 2015, Paper Th5C.2.

[10] K. Igarashi, D. Souma, Y. Wakayama, K. Takeshima, Y. Kawaguchi, T. Tsuritani, I. Morita, and M. Suzuki, "114 space-division-multiplexed transmission over 9.8-km weakly-coupled-6-mode uncoupled-19-core fibers," presented at the Optical Fiber Communication Conf., Los Angeles, CA, USA, 2015, Paper Th5C.4.

[11] B. J. Puttnam, R. S. Luís, W. Klaus, J. Sakaguchi, J.-M. Delgrado Mendinueta, Y. Awaji, N. Wada, Y. Tamura, T. hayashi, M. Hirano, and J. Marciante, "2.15 Pbs/transmission using a core homogeneous singlemode multi-core fiber and wideband optical comb," presented at the Eur. Conf. Exhib. Optical Communication, Valencia, Spain, 2015, Paper PDP.3.1.

[12] D. Soma, K. Igarashi, Y. Wakayama, T. Takashima, Y. Kawaguhi, N. Yoshikane, T. Tsuritani, I. Morita, and M. Suzuki, "2.05 Peta-bit/s Super Nyquist-WDM transmission using 9.8-km 6-Mode 19-core fiber in full C band," presented at the Eur. Conf. Exhib. Optical Communication, Valencia, Spain, 2015, Paper PDP.3.2.

[13] R. Ryf, H. Chen, N. K. Fontaine, A. M. Velazquez-Benítez, J. Antonio-López, C. Jin, H. Huang, M. Bigot-Astruc, D. Molin, F. Achten, P. Sillard, and R. Amezcua-Corea, "10-mode mode division multiplexed transmission over 125-km single-span multimode fiber," presented at the Eur. Conf. Exhib. Optical Communication, Valencia, Spain, 2015, Paper PDP.3.3.

[14] Y. Amma, Y. Sasaki, K. Takenaga, S. Matsuo, J. Tu, K. Saitoh, M. Koshiba, T. Morioka, and Y. Miyamoto, "High-density multicore fiber with heterogeneous core arrangement," presented at the Optical Fiber Communication Conf., Los Angeles, CA, USA, 2015, Paper Th4C.4.

[15] Y. Sasaki, S. Saitoh, Y. Amma, K. Takenaga, S. Matsuo, K. Saitoh, T. Morioka, and Y. Miyamoto, "Quasi-single-mode homogeneous 31-core fiber," presented at the Eur. Conf. Exhib. Optical Communication, Valencia, Spain, 2015, Paper We.1.4.4.

[16] P. Sillard, D. Molin, B. Bigot-Astruc, A. Amezcua-Correa, K. De Jongh, and F. Achten, "50μm multimode fibers for mode division multiplexing," presented at the Eur. Conf. Exhib. Optical Communication, Valencia, Spain, 2015, Paper Mo.4.1.2.

[17] T. Sakamoto, T. Matsui, K. Saitoh, S. Saitoh, K. Takenaga, S. Matsuo, Y. Tobita, N. Hanzawa, K. Nakajima, and F. Yamamoto, "Few-mode multi-core fiber with highest core multiplicity factor," presented at the Eur. Conf. Exhib. Optical Communication, Valencia, Spain, 2015, Paper We.1.4.3.

[18] S. Matsuo, K. Takenaga, K. Saitoh, K. Nakajima, Y. Miyamoto, and T. Morioka, "High-spatial-multiplicity multi-core fibres for future dense-space-division-multiplexing system," presented at the Eur. Conf. Exhib. Optical Communication, Valencia, Spain, 2015, Paper Th.1.2.1.

[19] S. Matsuo, K. Takenaga, Y. Arakawa, Y. Sasaki, S. Taniagwa, K. Saitoh, and M. Koshiba, "Large-effective-area ten-core fiber with cladding diameter of about 200 μm," *Opt. Lett.*, vol. 36, no. 23, pp. 4626–4628, Dec. 2011.

[20] D. Marcuse, "Loss analysis of single-mode fiber splices," *Bell Syst. Tech. J.*, vol. 56, no. 5, pp. 703–718, May 1977.

[21] Y. Amma, A. Takahashi, K. Takenaga, and S. Matsuo, "Accuracy of core alignment with end-view function for multicore fiber," presented at the IEEE Photonics Society Summer Topical Meeting Ser., Montreal, QC, Canada, Jul. 2014, Paper TuE2.4,.

[22] K. Yoshida, A. Takahashi, T. Konuma, K. Yoshida, and S. Sasaki. (2012, Jan.). Fusion splicer for specialty optical fiber with advanced functions.

Fujikura Tech. Rev. [Online]. 41, pp. 10–13. Available: http://www.fujikura.co.jp/eng/rd/gihou/backnumber/pages/2036771_4995.html

[23] T. Sakamoto, T. Mori, T. Yamamoto, M. Wada, and F. Yamamoto, "Moderately coupled 125-μm cladding 2 LP-mode 6-core fiber for realizing low MIMO-DSP and high spatial density," presented at the Eur. Conf. Exhib. Optical Communication, Cannes, France, 2015, Paper Tu.4.1.3.

[24] P. Winzer, A. Gnauck, A. Konczykowska, F. Jorge, and J.-Y. Dupuy, "Penalties from in-band crosstalk for advanced optical modulation formats," presented at the 37th Eur. Conf. Expo. Optical Communications, Geneva, Switzerland, Paper Tu.5.B.7.

[25] K. Takenaga, Y. Sasaki, N. Guan, S. Matsuo, M. Kasahara, K. Saitoh, and M. Koshiba, "Large effective-area few-mode multicore fiber," *Opt. Lett.*, vol. 24, no. 21, pp. 1941–1944, Nov. 1, 2012.

[26] K. Saitoh, M. Koshiba, K. Takenaga, and S. Matsuo, "Crosstalk and core density in uncoupled multicore fiber," *IEEE Photon. Technol. Lett.*, vol. 24, no. 21, pp. 1898–1901, Nov. 1, 2012.

[27] T. Mori, T. Sakamoto, M. Wada, T. Yamamoto, and F. Yamamoto, "Few-mode fibers supporting more than two lp modes for mode-division-multiplexed transmission with MIMO DSP," *J. Lightw. Technol.*, vol. 32, no. 14, pp. 2468–2479, Jul. 2014.

[28] T. Sakamoto, T. Mori, T. Yamamoto, and S. Tomita, "Differential mode delay managed transmission line for WDM-MIMO system using multi-step index fiber," *J Lightw. Technol.*, vol. 30, no. 17, pp. 2783–2787, Jul. 2012.

[29] K. Saioth and S. Matsuo, "Multicore fiber technology," *J. Lightw. Technol.*, vol. 36, no. 4, Feb. 2016, early access, doi:10.1109/JLT.2015.2466444

[30] M. Koshiba, K. Saitoh, and Y. Kokubun, "Heterogeneous multi-core fibers: Proposal and design principle," *IEICE Electron. Exp.*, vol. 6, no. 2, pp. 98–103, Jan. 2009.

[31] T. Hayashi, T. Taru, O. Shimakawa, T. Sasaki, and E. Sasaoka, "Design and fabrication of ultra-lows crosstalk and low-loss multi-core fiber," *Opt. Exp.*, vol. 19, no. 17, pp. 16576–16592, Aug. 2011.

[32] M. Koshiba, K. Saitoh, K. Takenaga, and S. Matsuo, "Analytical expression of average power-coupling coefficients for estimating intercore crosstalk in multicore fibers," *Photon. J.*, vol. 4, no. 5, pp. 1987–1995, Oct. 2012.

[33] K. Saitoh, M. Koshiba, K. Takenaga, and S. Matsuo, "Low-crosstalk multi-core fibers for long-haul transmission," presented at the Photonics West, San Francisco, CA, USA, 2012, vol. 8284, pp. 828401-1–828401-8.

[34] Y. Sasaki, Y. Amma, K. Takenaga, S. Matsuo, K. Saitoh, and M. Koshiba, "Investigation of crosstalk dependencies on bending radius of heterogeneous multicore fiber," presented at the Optical Fiber Communication Conf./ Nat. Fiber Optic Engineers Conf., Anaheim, CA, USA, 2013, Paper OTh3K.3

[35] K. Takenaga, Y. Arakawa, Y. Sasaki, S. Tanigawa, S. Matsuo, K. Saitoh, and M. Koshiba, "A large effective area multi-core fiber with an optimized cladding thickness," *Opt. Exp.*, vol. 19, no. 26, pp. B543–B550, Dec. 2011.

[36] T. Hayashi, T. Taru, O. Shimakawa, T. Sasaki, and E. Sasaoka, "Characterization of crosstalk in ultra-low-crosstalk multi-core fiber," *J. Lightw. Technol.*, vol. 30, no. 4, pp. 583–589, Feb. 2012.

[37] F. Yaman, S. Zhang, Y. Huang, E. Ip, J. D. Downie, W. A. Wood, A. Zahkharian, S. K. Mishra, J. E. Hurley, Y. Zhang, I. B. Djordjevic, M. Huang, E. Ateo, K. Nakamura, T. Inoue, Y. Inada, and T. Ogata, "First quasi-single-mode transmission over transoceanic distance using few-mode fibers," presented at the Optical Fiber Communication Conf., Los Angeles, CA, USA, 2015, Paper Th5C.7.

[38] Q. Sui, H. Zhang, J. D. Downie, W. A. Wood, J. Hurley, S. Mishra, A. P. T. Lau, C. Lu, H. Tam, and P. K. A. Wai, "Long-haul quasi-single-mode transmissions using few-mode fiber in presence of multi-path interference," *Opt. Exp.*, vol. 23, no. 3, pp. 3156–3169, Feb. 2015.

[39] A. Sano, H. Takara, T. Kobayashi, and Y. Miyamoto, "Crosstalk-managed high capacity long haul multicore fiber transmission with propagation-direction interleaving," *J. Lightw. Technol.*, vol. 32, no. 16, pp. 2771–2779, Aug. 2014.

[40] Y. Sasaki, Y. Amma, K. Takenaga, S. Matsuo, K. Saitoh, and M. Koshiba, "Few-mode multicore fiber with 36 spatial modes (three modes (LP$_{01}$, LP$_{11a}$, LP$_{11b}$) × 12 Cores)," *J. Lightw. Technol.*, vol. 33, no. 5, pp. 964–970, Mar. 2015.

[41] R. R. Thomson, H. T. Bookey, N. D. Psaila, A. Fender, S. Campbell, W. N. MacPherson, J. S. Barton, D. T. Reid, and A. K. Kar, "Ultrafast-laser inscription of a three dimensional fan-out device for multicore fiber coupling applications," *Opt. Exp.*, vol. 15, no. 18, pp. 11691–11697, Sep. 2007.

Shoichiro Matsuo (M'11) was born in Fukuoka, Japan, in 1964. He received the B.E. and M.E. degrees in electrical engineering from Kyushu University, Fukuoka, Japan, in 1988 and 1990, and the Ph.D. degree in production and information science from Utsunomiya University, Tochigi, Japan, in 2008, respectively.

He has been with Fujikura, Ltd., Chiba, Japan, since 1990, focusing on the research and development of transmission fibers for long-haul networks and FTTH networks as well as rare-earth-doped fibers and photonic bandgap fibers, and the manufacturing technology for these optical fibers. He was the General Manager of Laboratory, Fujikura, Ltd., from April 2013 to October 2015. He is currently the General Manager of both the Optical Fiber Development Department and the Suzuka Optical Fiber Production Department, Fujikura Ltd.

Dr. Matsuo is a Member of the Optical Society of America, the Japanese Society of Applied Physics, and the Institute of Electronics, Information and Communication Engineers.

Katsuhiro Takenaga was born in Tochigi, Japan, in 1976. He received the B.S. degree from Shinshu University, Nagano, Japan, and the M.S. degree from Hokkaido University, Sapporo, Japan, in 1999 and 2001, both in physics.

In 2001, he joined Fujikura, Ltd., Chiba, Japan, where he has been involved in research and development of optical fibers. He is a Member of the Institute of Electronics, Information and Communication Engineers of Japan.

Yusuke Sasaki was born in Chiba, Japan, in 1986. He received the B.E. and M.E. degrees in electrical engineering from the Tokyo Institute of Technology, Tokyo, Japan, in 2008 and 2010, respectively.

Since 2010, he has been with the Optics and Electronics Laboratory, Fujikura, Ltd., Chiba, where he has been involved in research and development of multicore fibers. He is a Member of the Institute of Electronics, Information and Communication Engineers of Japan.

Yoshimichi Amma received the B.S. degree in 2010 and M.S. degree in mechanical engineering from Yokohama National University, Kanagawa, Japan, in 2012.

He joined the Optical Fibre Technology Department, Optics and Electronics Laboratory, Fujikura, Ltd., Chiba, Japan, in 2012. He has three years of experience in research and development of multicore fibers, and he has attended six conferences.

Mr. Amma is a Member of the Institute of Electronics, Information and Communication Engineers of Japan.

Shota Saito was born in Hokkaido, Japan, in 1990. He received the B.S. degree in engineering and the M.S. degree in media and network technologies from Hokkaido University, Sapporo, Japan, in 2012 and 2014, respectively.

He has been at Fujikura, Ltd., Chiba, Japan, since 2014 and has been working on research and development of multicore fibers.

Mr. Saito is a Member of the Institute of Electronics, Information and Communication Engineers of Japan.

Kunimasa Saitoh (S'00–M'01) received the B.S., M.S., and Ph.D. degrees in electronic engineering from Hokkaido University, Sapporo, Japan, in 1997, 1999, and 2001, respectively.

From 1999 to 2001, he was a Research Fellow of the Japan Society for the Promotion of Science. From 2001 to 2005, he was a Research Associate with the Graduate School of Engineering, Hokkaido University. From 2005 to 2013, he was an Associate Professor with the Graduate School of Information Science and Technology, Hokkaido University, and in 2013, he became a Professor there. He has been involved in research on fiber optics, nanophotonics, integrated optical devices, and computer-aided design and modeling of guided-wave devices. He has authored more than 160 research papers in refereed international journals and 200 refereed conference presentations.

Dr. Saitoh is a Member of the Optical Society of America, and the Institute of Electronics, Information and Communication Engineers (IEICE). He received the Excellent Paper Award and the Young Scientist Award from the IEICE, in 1999 and 2002, respectively, the Young Scientists' Prize of the Commendation for Science and Technology from the Ministry of Education, Culture, Sports, Science, and Technology, Government of Japan, in 2008. From 2009 to 2010, he served as a Secretary/Treasurer of the IEEE Sapporo Section.

Takashi Matsui, biography not available at the time of publication.

Kazuhide Nakajima, biography not available at the time of publication.

Takayuki Mizuno (M'04) received the B.E. degree in applied physics, the M.E. degree in crystalline materials science, and the Dr. Eng. degree in quantum engineering from Nagoya University, Nagoya, Japan, in 1998, 2000, and 2007, respectively.

In 2000, he joined NTT Photonics Laboratories, NTT Corporation, Tokyo, Japan, where he was involved in research and development of silica planar lightwave circuit optical waveguide devices, including arrayed-waveguide gratings, Mach–Zehnder interferometer-based filters and switches, and digital coherent demodulators for advanced modulation formats. He is currently a Senior Research Engineer at NTT Network Innovation Laboratories, NTT Corporation, Kanagawa, Japan. He is the author and/or coauthor of more than 80 journal and international conference papers, and holds more than 30 granted patents. His present research interests include space-division multiplexed transmission technology for ultrahigh capacity optical transport systems.

Dr. Mizuno is a Member of the Institute of Electronics, Information, and Communication Engineers of Japan.

Hidehiko Takara received the B.S., M.E., and Ph.D. degrees in electrical engineering from the University of Keio, Kanagawa, Japan, in 1986, 1988, and 1997, respectively.

In 1988, he joined NTT Corporation, Kanagawa, Japan. Since then, he has been involved in research on ultrahigh-speed/large capacity optical transmission systems and optical measurement techniques. He is currently a Professor at the Okinawa National College of Technology, Nago, Japan. He is a Member of the Institute of Electronics, Information and Communication Engineers.

Yutaka Miyamoto, biography not available at the time of publication.

Toshio Morioka was born in Hyogo, Japan. He received the B.E. degree in applied physics from Waseda University, Tokyo, Japan, in 1982, the M.S. degree in optical sciences from the Optical Sciences Center, University of Arizona, Tucson, AZ, USA, in 1984, and the M.S. and Ph.D. degrees in physics and applied physics from Waseda University in 1985 and 1995, respectively. He joined the Yokosuka Electrical Communication Laboratory of Nippon Telegraph and Telephone Corporation (NTT) in 1985. From 1996 to 1999, he was with NTT Bureau de Genève, Switzerland. In 2011, he moved to DTU Fotonik, Kgs. Lyngby, Denmark, and has been a Full Professor since 2013. Since 1985, he has been involved in various pioneering research programs on ultrafast and ultrahigh capacity transmission technologies. In 1987, he demonstrated the first ultrafast all-optical demultiplexing of optical time-division multiplexing signals, which led to the first one Tbit/s transmission experiment in 1996. In 1993, he also initiated research on supercontinuum sources for ultrahigh capacity wavelength-division multiplexing systems. In 2008, he organized the EXtremely Advanced Transmission Initiative in Japan, to initiate space-division multiplexing research based on novel fibers (multicore/few-mode fibers) aiming at well over Pbit/s transmission, which led to the first one Pbit/s transmission experiment in 2012.

He received the IEE Electronics Letters Premium Award in 1997 for his first Tbit/s optical transmission. He is a Fellow of the Optical Society of America (OSA) and the Institute of Electronics, Information and Communication Engineers (IEICE) of Japan and a Member of the IEEE Photonics Society/Communications Society. He was a Program and General Cochair of the OSA Topical meeting on Nonlinear Guided Waves and Their Applications in 1995 and 1996, respectively. He served as the Editor-in-Chief of the IEICE Transactions on Communications in 2005–2006. He holds 60 granted patents.